Light diffraction by large amplitude ultrasonic waves in liquids

Laszlo Adler,[a] John H. Cantrell,[b] and William T. Yost[b]

[a]Adler Consultants Inc./ Ohio State University, Columbus, Ohio, USA
[b]NASA Langley Research Center, Hampton, Virginia, USA

Abstract. Light diffraction from ultrasound, which can be used to investigate nonlinear acoustic phenomena in liquids, is reported for wave amplitudes larger than that typically reported in the literature. Large amplitude waves result in waveform distortion due to the nonlinearity of the medium that generates harmonics and produces asymmetries in the light diffraction pattern. For standing waves with amplitudes above a threshold value, subharmonics are generated in addition to the harmonics and produce additional diffraction orders of the incident light. With increasing drive amplitude above the threshold a cascade of period-doubling subharmonics are generated, terminating in a region characterized by a random, incoherent (chaotic) diffraction pattern. To explain the experimental results a toy model is introduced, which is derived from traveling wave solutions of the nonlinear wave equation corresponding to the fundamental and second harmonic standing waves. The toy model reduces the nonlinear partial differential equation to a mathematically more tractable nonlinear ordinary differential equation. The model predicts the experimentally observed cascade of period-doubling subharmonics terminating in chaos that occurs with increasing drive amplitudes above the threshold value. The calculated threshold amplitude is consistent with the value estimated from the experimental data.

INTRODUCTION. In 1932, Debye and Sears [1] in the USA and Lucas and Biquard [2] in France independently observed that when a monochromatic light beam propagates perpendicularly through an ultrasonic beam, the light will diffract into several orders. A theoretical model, developed by Raman and Nath [3] (the Raman-Nath theory), shows that the ultrasonic wave behaves like a diffraction grating for the light. Starting with the electromagnetic wave equation and introducing a variable refractive index μ for the light due to ultrasonic pressure variations, they predicted the intensity of each order as well as the positions of the orders. The intensity I_n of the diffracted light in the nth order is given as

$$I_n=J_n^2(\nu) \tag{1}$$

where J_n is the nth order Bessel function and ν is the Raman-Nath parameter given as

$$\nu=2\pi\mu a/\lambda \tag{2}$$

where a is the width of the sound field and λ is the wavelength of the light. The angle Θ of the diffracted light is obtained as [3]

$$\sin(\Theta)= n\lambda/\lambda^* \tag{3}$$

where λ^* is the wavelength of the sound. The Raman-Nath theory is in good agreement with the experimental results for infinitesimal amplitude ultrasonic waves, since the intensity of the orders for such case is proportional to the square of Bessel functions.

Zankel and Hiedemann [4] observed that finite (large) amplitude ultrasonic waves produce an asymmetry in the diffraction pattern resulting from the nonlinearity of the propagation medium, which progressively distorts the ultrasonic sinusoidal waveform along the propagation path. The asymmetry in the first orders (the difference in the negative and positive order) of the measured light intensity increases with the fundamental wave pressure. The asymmetry in the diffraction pattern also increases with an increase in the wave propagation distance as illustrated in Fig.1.

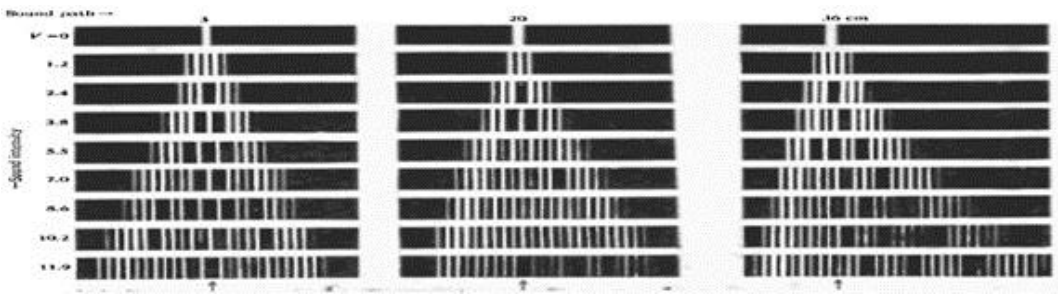

Figure 1. Light diffraction by ultrasonic waves in water with frequency of 1.76 MHz at 3, 20 and at 36 cm. (Reproduced with permission from M.A. Breazeale, J. Acoust. Soc. Am. **33,** 857 (1961). Copyright, Acoustical Society of America)

The asymmetry in the light diffraction orders due to the generated acoustic second harmonics allowed a determination of the nonlinearity parameter B/A for water and m-Xylene by Adler and Hiedemann [6]. It was later observed that above a threshold

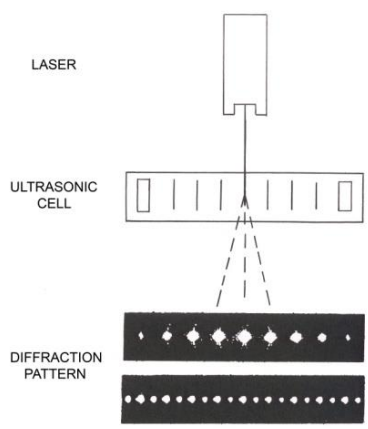

Figure 2. Schematic diagram of the diffraction pattern below the threshold (top pattern) and above threshold (bottom pattern).

acoustic drive amplitude subharmonics are generated, leading to diffraction orders in addition to the orders from the integer harmonics [7,8]. The additional diffraction orders generated above the acoustic threshold amplitude are shown in the bottom diffraction pattern of Fig.2. In the present paper a toy model is introduced to quantify the threshold acoustic drive amplitude necessary to generate in a liquid-filled resonant cavity a cascade

of period-doubling subharmonics that, with increasing drive amplitude, terminates in chaos. Theoretical predictions from the model are compared to experiment.

ACOUSTIC HARMONIC GENERATION UNDER RESONANT CONDITIONS. Consider acoustic wave propagation in a dissipative medium having quadratic nonlinearity. The equation governing longitudinal wave propagation along the spatial direction x can be approximated in Lagrangian coordinates as [9]

$$\frac{\partial^2 u}{\partial t^2} = c^2 \frac{\partial^2 u}{\partial x^2} + \lambda_a \frac{\partial^3 u}{\partial t \partial x^2} - \beta c^2 \frac{\partial u}{\partial x}\frac{\partial^2 u}{\partial x^2} \tag{4}$$

where u is the particle displacement, t is time, c is the acoustic phase velocity, λ_a is the damping coefficient, and $\beta = (B/A) + 2$ is the nonlinearity parameter for liquids, where A and B are the Beyer coefficients. The solution of Eq.(4) to second harmonic terms (neglecting the static term), assuming a driving source $u(0,t) = \eta_0 \cos(\omega t)$, is given as [9]

$$u = \eta_0\, e^{-\alpha_1 x}\cos(\omega t - kx) - \frac{1}{8}\beta k^2 \eta_0^2 \left[\frac{\exp(-2\alpha_1 x) - \exp(-\alpha_2 x)}{\alpha_2 - 2\alpha_1}\right] \sin 2(\omega t - kx) + \cdots \tag{5}$$

where $k = \omega/c$, $\alpha_1 \approx \omega^2\lambda/2c^3$ is the fundamental wave attenuation coefficient, and α_2 is the second harmonic attenuation coefficient related to α_1 by the constant $R_r = \alpha_2/\alpha_1$.

Now consider a fluid-filled cavity formed between parallel surfaces of a flat transducer and a flat reflector. The 'propagating wave' model [10] is used to assess the effects of continuous waves reflecting normally between parallel surfaces of a resonant cavity [11]. For continuous waves bounded by reflecting surfaces at $x = 0$ and $x = L/2$ the amplitude at a point $x \in [0, L/2]$ consists of the sum of all contributions resulting from waves which had been generated at the point $x = 0$ and have propagated to the point x. The fundamental wave resonant amplitude $(\eta_1)_{res}$ is obtained as [11]

$$(\eta_1)_{res} = |Re[\bar{A}_1(x,t)]| \approx \frac{\eta_0}{\alpha_1 L} \ . \tag{6}$$

The second harmonic resonant amplitude $(\eta_2)_{res}$ is obtained as [11]

$$(\eta_2)_{res} = \frac{1}{16}\frac{\beta k^2 \eta_0^2}{R_r \alpha_1^2 L} \ . \tag{7}$$

TOY MODEL FOR ASSESSING SUBHARMONIC GENERATION AND CHAOS. The linear wave equation $\partial^2 u/\partial t^2 - c^2\, \partial^2 u/\partial x^2 = 0$ is a partial differential equation (PDE) that, for unforced resonant conditions at a point $x \in [0, L/2]$, can be reduced to the linear ordinary differential equation (ODE) $d^2\eta/dt^2 + \omega_0^2\eta = 0$, where $\omega_0 = 2\pi c/L$, by substituting $u(x,t) = \eta(t)\cos kx$ in the wave equation. The solution to the ODE governs the resonant amplitude for any $x \in [0, L/2]$. The differential equation obtained by eliminating the dependence on at least one independent variable in the PDE is an example of a toy model. Consider the equation

$$\frac{d^2\eta}{dt^2} + \gamma\frac{d\eta}{dt} + \omega_0^2\eta - \frac{3}{8}\beta\frac{\omega^4 L}{R_r c^2}\eta^2 = \frac{\omega^2}{2\pi}\eta_0\cos\omega t \qquad (8)$$

where $\gamma = c\alpha_1$. It is assumed that Eq.(8) will adequately serve as a toy model for possible subharmonic solutions of Eq.(4), providing that Eq.(8) correctly predicts the fundamental and second harmonic resonant amplitudes given by Eqs.(6) and (7), respectively. A perturbation solution to Eq.(8) has been shown to yield the appropriate amplitudes [11].

In nonlinear systems with oscillatory drive forces the generation of higher harmonics of order n = 2, 3, ··· serves to stimulate and sustain the generation of subharmonics of fractional order 1/n [12]. For an acoustic resonant system subharmonic generation occurs when the amplitude of excitation attains a threshold value dependent on the acoustic drive frequency and attenuation in the medium. The driving term $(\omega^2\eta_0/2\pi)\cos(\omega t)$ in Eq.(8) allows the possibility of stable subharmonic generation leading to chaos. An assessment of this possibility can be obtained by testing for homoclinic bifurcation (subharmonic generation) using the Melnikov method [12].

The Melnikov method establishes conditions under which subharmonic generation leading to chaos is assured. Central to the method is the Melnikov function $M(t_0)$ [12], which for Eq.(8) is [11]

$$M(t_0) = \int_{-\infty}^{\infty}\xi_{hp}(t-t_0)h[\eta_{hp}(t-t_0),\xi_{hp}(t-t_0),t]\,dt \qquad (9)$$

where $h[\eta_{hp}(t-t_0),\xi_{hp}(t-t_0),t] = \left(\frac{\omega^2}{2\pi}\eta_0\cos\omega t - \gamma\xi_{hp}(t-t_0)\right)$ and $\xi_{hp}(t-t_0) = \frac{2R_r c^2\omega_0^3}{\beta L\omega^4}\frac{\sinh[\omega_0(t-t_0)/2]}{\cosh^3[\omega_0(t-t_0)/2]}$. Evaluation of the integrals yields [11]

$$M(t_0) = \frac{8R_r c^2\cos\omega t_0}{\beta L\sinh(\omega\pi/\omega_0)}\eta_0 - \frac{128}{15}\frac{R_r^2 c^5\omega_0^5}{\beta^2 L^2\omega^8}\alpha_1 \quad . \qquad (10)$$

The vanishing of $M(t_0)$ marks the beginning of an unstable region in phase space that includes both subharmonic generation and chaos. For given values of the attenuation coefficient α_1 and drive frequency ω, the drive amplitude threshold $(\eta_0)_{th}$ necessary for $M(t_0) = 0$ is obtained for a value of t_0 such that $\cos(\omega t_0) = 1$ in Eq.(10). Thus, from Eq.(10) the threshold drive amplitude necessary to initiate a cascade of period-doubling subharmonics that with increasing drive amplitude terminates in chaos is

$$(\eta_0)_{th} = \frac{16}{15}\frac{R_r c^3}{\beta L}\left(\frac{\omega_0^5}{\omega^8}\right)\alpha_1\sinh\left(\frac{\omega\pi}{\omega_0}\right) \quad . \qquad (11)$$

EXPERIMENTS AND CONCLUSION. The predictions of Eq.(11) are compared to measurements obtained for a water-filled resonant cavity [13]. For water $c \approx 1.54 \times 10^3$ m s^{-1}, $\beta \approx 6.8$, and $R_r \approx 4$. In the present experiments $\omega = \omega_0 = 31.4$ MHz, $\alpha_1 \approx 0.127$ m^{-1}, and $L = 0.06$ m. The threshold displacement drive amplitude $(\eta_0)_{th}$ necessary for subharmonic generation is calculated by substituting these values in Eq.(11) to obtain $(\eta_0)_{th} \approx 1.9\times10^{-12}$ m. This drive amplitude results in the fundamental resonant amplitude $(\eta_1)_{res} \approx 0.2$ nm as calculated from Eq.(6). The resonant amplitude corresponding to subharmonic generation is estimated in the present experiments to be roughly 0.3 nm. The calculated

value $(\eta_1)_{res} \approx 0.2$ nm is consistent with the experimental value. As the acoustic drive amplitude is further increased, the subharmonic pattern transitions via a cascade of period-doublings to random, chaotic oscillations, as predicted by the Melnikov method. Fig.3a shows the predicted chaotic diffraction pattern. Fig.3b, however, shows a diffraction pattern for drive amplitudes beyond chaos corresponding to the occurrence of a stable subharmonic not quantitatively predicted by the present model and is the subject of further investigation.

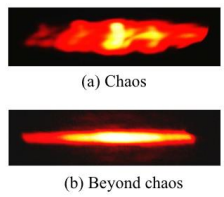

Figure 3. Acousto-optic diffraction patterns for larger transducer drive amplitudes: (a) chaotic region; (b) stable subharmonic beyond chaos (from L. Adler, W. T. Yost, and J. H. Cantrell, AIP Conf. Proc. **1433**, 527 (2012)).

ACKNOWLEDGMENT. This work was supported by the Advanced Composites Project, NASA Langley Resech Center, Hampton, Virginia, USA, and an Emeritus Academy Grant, Ohio State University, Columbus, Ohio, USA.

REFERENCES

1. P. Debye, F.W. Sears, Proc. Nat.Acad.Sci.**18**, 409 (1932).
2. R. Lucas, P.J. Biquard, Physique Radium **194**, 2132 (1932).
3. C.V. Raman, N.S. Nath, Pro. Ind. Ac. Sci. **2**, 406 (1935).
4. K.L. Zankel, E.A. Hiedemann, *J. Acoust. Soc. Am.* ***31,*** *1366 (1959).*
5. M.A. Breazeale, J. Acoust. Soc. Am. **33,** 857 (1961).
6. L. Adler, E.A. Hiedemann, J. Acoust. So. Am. **34,** 410 (1962).
7. A. Korpel, R. Adler, Appl. Phys. Lett. **7**, 106 (1965).
8. L. Adler, M.A. Breazeale, Die Naturwissenschaften **8**, 385 (1968).
9. J. H. Cantrell, "Fundamentals and applications of nonlinear ultrasonic nondestructive evaluation," in *Ultrasonic and Electromagnetic NDE for Structure and Material Characterization*, edited by T. Kundu (Taylor and Francis, London, 2012) p. 395.
10. D. I. Bolef, J. G. Miller, "High-frequency continuous wave ultrasonics," in *Physical Acoustics, Vol. VIII*, edited by W. P. Mason and R. N. Thurston (Academic, New York, 1971) p. 95.
11. J. H. Cantrell, L. Adler, W. T. Yost, Chaos **25**, 023115 (2015).
12. D. W. Jordon, P. Smith, *Nonlinear Ordinary Differential Equations* (Oxford University Press, New York, 2007).
13. L. Adler, W. T. Yost, and J. H. Cantrell, "Subharmonics, chaos and beyond," AIP Conf. Proc. **1433**, 527 (2012).